



PERGAMON

International Journal of Solids and Structures 39 (2002) 3831–3844

INTERNATIONAL JOURNAL OF
SOLIDS and
STRUCTURES

www.elsevier.com/locate/ijsolstr

Steady shear and thermal run-away in clayey gouges

I. Vardoulakis *

Department of Mechanics, Faculty of Applied Sciences, National Technical University of Athens, 5 Heroes of Polytechnion Avenue, Zografou, Athens 157 73, Greece

Received 15 August 2001; received in revised form 28 November 2001

Abstract

In the present paper we study the thermo-viscoplastic coupling in clayey fault-gouges under shear. It is shown that steady shear for a strain-rate hardening/thermally softening clay is only then possible, if the ambient temperature is less than some well-defined critical value. Past this critical temperature the balance between the two antagonistic mechanisms of viscous strengthening and thermal softening cannot be sustained and may result in dynamic (catastrophic) shear deformation. © 2002 Elsevier Science Ltd. All rights reserved.

Keywords: Shear deformation; Continuum; Mechanics; Geomechanics

1. Introduction

All formulations of problems referring to deformation must observe the basic balance laws of continuum mechanics. In most applications in Geomechanics we will resort mainly to mass balance and momentum balance. However for the analysis of catastrophic events like landslides, mudflows, rapid fault shearing, etc. we must include energy considerations as well (cf. Habib, 1967; Anderson, 1980; Voight and Faust, 1982; Mase and Smith, 1985; Vardoulakis, 2000, 2002).

Although it is believed that balance laws have general validity, we should emphasize here that there are many examples, which are indicating that the formulation of balance laws in continuous media include implicitly important constitutive assumptions as well. In the present paper we will discuss, the energy balance equation as this is formulated and applied to thermo-hydro-mechanically coupled deformations of water-saturated porous materials like a clayey fault-gouge. The formulation of the energy balance equation in that particular setting is neither an obvious nor a formal task. Here we attempt such a formulation by postulating a unique temperature field for both constituents, namely the solid and the aqueous phases.

In the fluid mechanics literature a thermal run-away instability is known to set in, when in a steady shear flow and at some critical ambient temperature the effect of strain-rate fails to counterbalance the effect of temperature (Gruntfest, 1963). This mechanism becomes clear by recalling for example Newton's law for the shear stress in a fluid ¹ accounting also for the temperature dependence of the fluid viscosity,

* Fax: +30-1-772-1302.

E-mail address: i.vardoulakis@mechan.ntua.gr (I. Vardoulakis).

¹ For water the shear-stress is given approximately by Eq. (1) with $\eta_{w0} = 1.467 \text{ cP}$ and $M = 0.0179 \text{ }^{\circ}\text{C}^{-1}$.

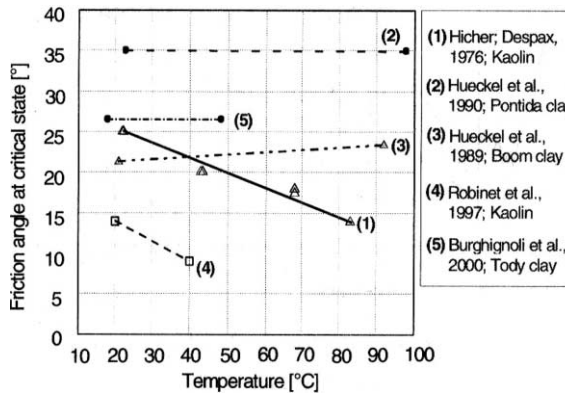


Fig. 1. The variation of the critical friction coefficient with temperature, after Laloui (2001).

$$\tau \approx \eta_{w0} e^{-M\theta} \dot{\gamma} \quad (1)$$

Thus past a critical temperature the imbalance between the two antagonistic mechanisms of viscous strengthening and thermal softening results inevitably in an accelerating (catastrophic) shear deformation.

In the soil mechanics literature there is ample reference to the fact that clays are strain-rate sensitive materials, the majority of which shows a strain-rate hardening behavior (Taylor, 1948; Sigh and Mitchell, 1968; Leinenkugel, 1976; Adachi and Oka, 1982). As a matter of fact clays are thermo-viscoplastic materials (Campanella and Michell, 1968; Nova, 1986; Hueckel and Baldi, 1990). As pointed out recently by Modaressi and Laloui (1997), as early as in the mid 1970s Hicher (1974) and Despax (1976) reported that some clays show thermoplastic softening behavior as far as their friction coefficient in the critical state is concerned (see Fig. 1 after Laloui, 2001).

Thus the friction angle at critical state for some clays is practically unaffected by temperature whereas for some other clays it is a decreasing function of temperature. These differences are attributed mainly to the clay mineralogy, which presumably influences the thermo-mechanical behavior of a clay in decisive manner (e.g. montmorillonite versus kaolinite).

Our analysis here applies to the poro-thermo-mechanical behavior of clayey fault gouges or to shear-bands inside thick clayey deposits. We will show that thermal run-away instabilities are quite probable to occur in clayey material as soon as the particular clay shows frictional strain-rate hardening and thermal softening, and the ambient temperature exceeds a well-defined critical value.

2. Energy balance in porous, fluid-saturated soils

Let $e = e(x_k, t)$, $P^{(m)} = P^{(m)}(x_i, t)$ and $Q_k = Q_k(x_i, t)$ be the specific internal energy the stress power of a water-saturated clayey material and the heat flux vector in this medium at any point and time. The local form of the energy balance of continuum mechanics reads as follows (cf. Vardoulakis and Sulem, 1995),

$$\rho \frac{D^{(m)} e}{Dt} = P^{(m)} - \frac{\partial Q_k}{\partial x_k} \quad (2)$$

where $D^{(m)}/Dt$ denotes the “barycentric” material derivative of the mixture

$$\frac{D^{(m)}}{Dt} = \frac{\partial}{\partial t} + v_i^{(m)} \frac{\partial}{\partial x_i}; \quad v_i^{(m)} = \frac{\rho^{(1)}}{\rho} v_i^{(1)} + \frac{\rho^{(2)}}{\rho} v_i^{(2)} \quad (3)$$

In Eq. (3) (second term) $v_i^{(\alpha)}(x_k, t)$ are the partial velocities of the constituents. In these expressions the superscript (1) denotes the solid phase, (2) the fluid phase and (m) the mixture. We recall that the partial densities are expressed in terms of the porosity n of the soil, the density ρ_s of the solids and the density ρ_w of the fluid (water)

$$\rho^{(1)} = (1 - n)\rho_s, \quad \rho^{(2)} = n\rho_w \quad (4)$$

The total density of the ‘mixture’ is

$$\rho = n\rho_w + (1 - n)\rho_s \quad (5)$$

We remark that the concept of partial stresses of the theory of mixtures is not meaningful in soil mechanics (Bishop and Skinner, 1977). Thus the total stress is decomposed, according to Tezaghi’s effective stress principle, into an effective stress and into a pore-water pressure

$$\sigma_{ij} = \sigma'_{ij} - p_w\delta_{ij} \quad (p_w > 0) \quad (\text{Compression is taken negative.}) \quad (6)$$

This means also that for the fluid phase we neglect viscosity. Moreover it is assumed that the effective stress is dual-in-energy to the rate of deformation of the solid phase and that the pore-water pressure works on the fluid volumetric strain-rate. Accordingly the stress power for the mixture is defined as

$$P^{(m)} \approx \sigma'_{ij}D_{ij}^{(1)} + p_wD_{kk}^{(2)} \quad (7)$$

where

$$D_{ij}^{(\alpha)} = \frac{1}{2} \left(\frac{\partial v_i^{(\alpha)}}{\partial x_j} + \frac{\partial v_j^{(\alpha)}}{\partial x_i} \right) \quad (\alpha = 1, 2) \quad (8)$$

denote the rate of deformation tensors for each constituent.

Furthermore we assume that the fluid phase is thermo-elastic and that the solid phase is thermo-elasto-visco-plastic. The last assumption is expressed by the decomposition of the rate of deformation of the solid phase into a reversible (elastic) and into a irreversible (visco-plastic) part,

$$D_{ij}^{(1)} = D_{ij}^e + D_{ij}^p \quad (9)$$

In order to evaluate further the energy balance Eq. (2) we postulate a unique temperature field $\theta(x_i, t)$ for both phases and we assume that the rate of internal specific energy of the mixture depends on changes in temperature and on the rate of elastic deformation,

$$\rho \frac{D^{(m)}e}{Dt} \approx j(\rho C)_m \frac{D^{(m)}\theta}{Dt} + \sigma'_{ij}D_{ij}^e + p_wD_{kk}^{(2)} \quad (10)$$

In the above expression $j = 4.2 \text{ J/cal}$ is the mechanical equivalent of heat and C_m is the specific heat of the mixture. Here we set

$$(\rho C)_m = (1 - n)\rho_s C_s + n\rho_w C_w \quad (11)$$

with $j\rho_s C_s$ and $j\rho_w C_w$ being the volumetric heat capacities of the solid and aqueous constituent, respectively (cf. Yu et al., 1999).

With these assumptions, the energy balance Eq. (2) becomes,

$$j(\rho C)_m \frac{D^{(m)}\theta}{Dt} = -\frac{\partial Q_k}{\partial x_k} + D \quad (12)$$

where

$$D = \sigma'_{ij}D_{ij}^p \quad (13)$$

corresponds only to the work dissipated by the deformation of the solid phase, since all dissipation in the fluid phase has been neglected.

Finally, as far as the heat flow is concerned, we assume the validity of Fourier's law

$$Q_i = -jk_m \frac{\partial \theta}{\partial x_i} \quad (14)$$

where k_m is the thermal conductivity of soil–water mixture

$$k_m = (1 - n)k_s + nk_w \quad (15)$$

In the above expression k_s and k_w are the thermal conductivities of the soil constituents.

With Fourier's law, Eq. (14), we obtain the following heat conduction equation

$$\frac{D^{(m)}\theta}{Dt} = \kappa_m \nabla^2 \theta + \frac{1}{j(\rho C)_m} D \quad (16)$$

where

$$\kappa_m = \frac{k_m}{(\rho C)_m} \quad (17)$$

is the coefficient of thermal diffusivity of the soil ² with dimensions $[\kappa_m] = L^2 T^{-1}$. We recall that the heat generation term is given by the dissipation function defined above through Eq. (13).

3. Steady shear of a long shear-band

We consider now the steady shear deformation of a 'long' band of water-saturated clayey material (e.g. an 'active'-fault gouge). We assume that the considered shear-band has the thickness d and that the various mechanical fields do not vary along its 'long' x -direction; they may vary along the 'short', z -direction. Under steady conditions momentum balance degenerates into static equilibrium, i.e. into constant shear stress across the shear-band

$$\frac{\partial \sigma_{xz}}{\partial z} = 0 \Rightarrow \sigma_{xz} = \tau_d = \text{const.} \quad (18)$$

We assume in addition that the shear-band material is at a 'critical state', deforming thus isochorically. With this assumption the components of the velocity vector inside the shear-band are

$$v_x^{(1)} = v(z), \quad v_y^{(1)} = v_z^{(1)} = 0 \quad (19)$$

For steady, isochoric shear deformation, mass balance together with Darcy's law results into a constant pore-pressure profile across the shear-band. This means that under steady conditions no flow is sustained across the shear-band. With $\theta = \theta(z)$ and Eqs. (19) this means in turn that in the considered case all convective terms in the material time derivative of the temperature field in Eq. (16) will vanish, and $D^{(m)}\theta/Dt = \partial\theta/\partial t$. Consequently under the given setting of steady (creeping) shear deformation the advection of heat by fluid into/out of the shear zone is null. Of course if steady creep breaks down, then, within a dynamic setting, heat advection may become significant. This scenario will not be addressed here.

² The index m denotes the solids–water mixture which makes-up a soil element.

For the considered steady shearing deformation the heat Eq. (16) yields to,

$$jk_m \frac{d^2\theta}{dz^2} + D = 0 \quad (20)$$

By neglecting elastic strains, the rate of mechanical work dissipated in heat is given by the work of the shear stress on the rate of shear deformation

$$D = \sigma_{xz} D_{xz}^p + \sigma_{zx} D_{zx}^p \approx \tau_d \dot{\gamma}, \quad \dot{\gamma} = \frac{\partial v}{\partial z} \quad (21)$$

For soil-like materials, the steady-state shear stress (i.e. the “strength” of the gouge) is given formally by a friction law

$$\tau_d = \tau_{cs} = \sigma'_n \mu_{cs} \quad (22)$$

In this expression σ'_n is the effective stress, acting normal to the shear-band. Since the pore-pressure is constant, then for constant total normal stress we get that σ'_n is also constant. Moreover in Eq. (22) μ_{cs} is the friction coefficient of the gouge at critical state. We assume here that the material is frictionally thermo-visco-plastic,

$$\mu_{cs} = \hat{\mu}(\dot{\gamma}, \theta) \quad (23)$$

In particular we assume here that the friction coefficient in the critical state is given by a strain-rate hardening power-law and a thermal softening exponential law as follows:

$$\mu_{cs} = g(\dot{\gamma}) \cdot f(\theta) = \mu_{ref} \cdot \left(\frac{\dot{\gamma}}{\dot{\gamma}_{ref}} \right)^N e^{-M(\theta-\theta_1)} \quad (24)$$

Accordingly the shear stress at critical state is given by a qualitatively similar expression as Newton's law Eq. (1)

$$\tau_{cs} = \left(\frac{\sigma'_n \mu_{ref}}{\dot{\gamma}_{ref}} \cdot \left(\frac{\dot{\gamma}}{\dot{\gamma}_{ref}} \right)^{N-1} \right) e^{-M(\theta-\theta_1)} \dot{\gamma} \quad (25)$$

The exponents M and N as well as the other model parameters appearing in the above empirical law must always be determined experimentally, say in temperature and velocity controlled ring-shear experiments. Strain-rate friction hardening is viewed here as the necessary counterbalancing effect to thermal softening. We notice however that if the clay shows instead a frictional strain-rate softening effect (cf. for example Tika and Hutchinson, 1999), then in the considered case (of thermal softening as well) no steady shear creep solution for the shear-band is possible.

From Eqs. (22)–(24) we get,

$$\tau_d = \tau_r(\dot{\gamma}) e^{-M(\theta-\theta_1)}, \quad \tau_r = \tau_{ref} \left(\frac{\dot{\gamma}}{\dot{\gamma}_{ref}} \right)^N, \quad \tau_{ref} = \sigma'_n \mu_{ref} \quad (26)$$

$$\dot{\gamma} = \dot{\gamma}_{ref} \left(\frac{\tau_r}{\tau_{ref}} \right)^{1/N} = \dot{\gamma}_0 e^{M(\theta-\theta_1)}, \quad \dot{\gamma}_0 = \left(\frac{\tau_d / \sigma'_n}{\mu_{ref}} \right)^{1/N} \dot{\gamma}_{ref} = \text{const.} \quad (27)$$

With this notation the dissipation is given in terms of the (constant) shear stress τ_d , the (constant) reference shear strain-rate, $\dot{\gamma}_0$, and in terms of an exponential function of the temperature

$$D \approx \tau_d \dot{\gamma} = D_0 e^{M(\theta-\theta_1)}, \quad D_0 = \tau_d \dot{\gamma}_0 \quad (28)$$

With this dissipation function, the governing Eq. (20) becomes,

$$jk_m \frac{d^2\theta}{dz^2} + D_0 e^{M(\theta - \theta_1)} = 0 \quad (29)$$

According to Fig. 2, we study here the possibility that the temperature at the boundaries has a constant value, equal to the ambient temperature

$$\theta(\pm d/2) = \theta_d = \text{const.} \quad (30)$$

Eq. (28) is non-dimensionalized by introducing as new variables

$$z^* = \frac{z}{d/2}, \quad \theta^* = M(\theta - \theta_1) \quad (31)$$

This transformation is yielding to the following non-linear, ordinary differential equation,

$$\frac{d^2\theta^*}{dz^{*2}} + \beta e^{\theta^*} = 0, \quad z^* \in [-1, 1] \quad (32)$$

with a single dimensionless physical parameter, the Gruntfest number,

$$\beta = \frac{M}{N} \frac{\tau_d \dot{\gamma}_0}{jk_m} \left(\frac{d}{2} \right)^2 \quad (33)$$

The analytical solution of the governing differential Eq. (32) can be found in mathematical textbooks (e.g. Kamke, 1977). This solution is given in terms of two integration constants, which according to Fig. 2 are identified from the symmetry condition,

$$\theta^*(0) = \theta_{\max}^*, \quad \left. \frac{d\theta^*}{dz^*} \right|_{z^*=0} = 0 \quad (34)$$

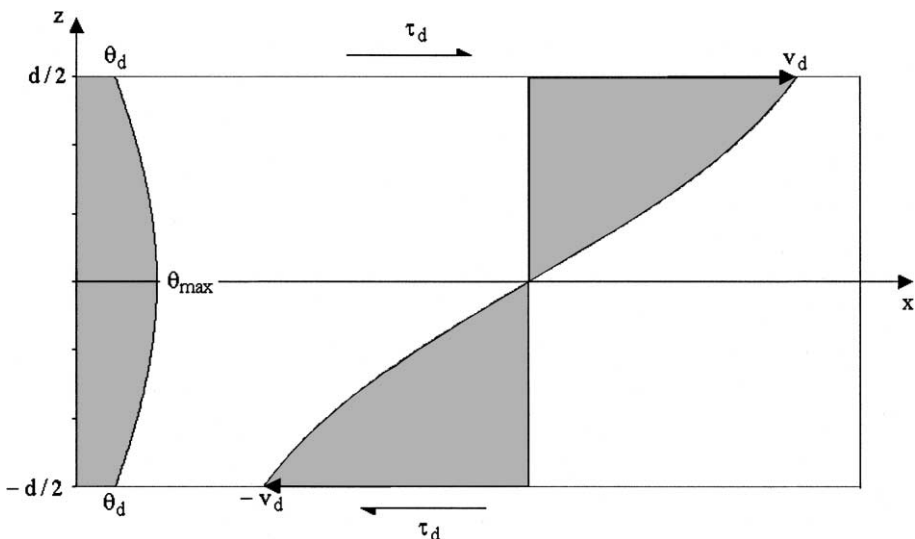


Fig. 2. Steady shearing of a long shear-band: in a thermo-viscoplastic material high velocity gradients counterbalance high temperatures resulting to constant shear stress across the band.

and the boundary condition

$$\theta^*(\pm 1) = \theta_d^* = \text{const.} \quad (35)$$

Accordingly the analytical solution of Eq. (32) becomes,

$$\theta^* = \theta_d^* - 2 \ln \left(\frac{\cosh \left(e^{\theta_d^*/2} \sqrt{\beta/2} z^* \right)}{\cosh \left(e^{\theta_d^*/2} \sqrt{\beta/2} \right)} \right) \quad (36)$$

With the solution, Eq. (36), the boundary condition (35) at $z^* = \pm 1$ yields

$$\theta_{\max}^* = \theta_d^* + 2 \ln \left(\cosh \left(e^{\theta_d^*/2} \sqrt{\beta/2} \right) \right) \quad (37)$$

Thus steady-shear is possible only if the above transcendental Eq. (37) for the maximum temperature θ_{\max}^* in the middle of the shear-band has a solution. This solution depends on the value of the temperature at the shear-band boundary θ_d^* and on the value of the Gruntfest number β . Accordingly, before we proceed further with the discussion of the transcendental Eq. (37), we must have an estimate of the Gruntfest number β .

4. Material and system parameters estimation

According to Eq. (33), the Gruntfest number β combines the following information:

- (a) The thermal conductivity of the soil k_m ; $[jk_m] = \text{FL}/(\text{Grad LT})$.
- (b) The ratio $m = M/N$ of the two hardening exponents; $[m] = 1/\text{Grad}$.
- (c) The shear-band (fault) thickness d ; $[d] = \text{L}$.
- (d) The in situ shear stress τ_d ; $[\tau_d] = \text{F/L}^2$.
- (d) The reference strain rate $\dot{\gamma}_0$; $[\dot{\gamma}_0] = 1/\text{T}$.

For estimating the thermal conductivity of the clay we used data provided by Yu et al. (1999). With $\kappa_m = 5.96 \times 10^{-7} \text{ m}^2/\text{s}$, $(\rho_w j C_w) = 4.18 \times 10^6 \text{ J}/(\text{°C m}^3)$, $(\rho_s j C_s) = 2.856 \times 10^6 \text{ J}/(\text{°C m}^3)$ and $n = 0.33$ taken from this reference we get $jk_m = 0.46 \text{ J}/(\text{°C m s})$. On the other hand, if we use the parameters that we selected for analyzing the Vajont landslide (Vardoulakis, 2002) we get $jk_m = 0.42 \text{ J}/(\text{°C m s})$. We assume here as a typical value, $jk_m = 0.45 \text{ J}/(\text{°C m s})$.

In order to estimate the strain-rate sensitivity exponent N we resorted to experimental results concerning a kaolin clay, reported by Leinenkugel (1976) (see Fig. 3), thus yielding $N \approx 0.01$.

For estimating the temperature sensitivity we used the data from Hicher (1974) (Fig. 4),

$$\mu_{cs} = \tan(22.3^\circ) \left(\frac{\dot{\gamma}}{\dot{\gamma}_0} \right)^N e^{-M(\theta - 22^\circ\text{C})}, \quad M \approx 0.0093 \text{ }^\circ\text{C}^{-1}, \quad \dot{\gamma}_0 = 1\%/\text{h} \quad (38)$$

Thus from Figs. 3 and 4 we get that for a rate- and temperature sensitive kaolin clay, $m \approx 1 \text{ }^\circ\text{C}^{-1}$. In the present analysis the exponent ratio $m = M/N$ will be varied between $m = 1 \text{ }^\circ\text{C}^{-1}$ and $m = 0.1 \text{ }^\circ\text{C}^{-1}$, in order to cover a possible range of behaviors between ‘strong’ and ‘weak’ thermal softening, respectively.

The shear-band thickness is also varied here between extremes, as $d = 0.1$ and 0.0015 m . The lower bound estimate for the shear-band thickness stems from an earlier publication by Morgenstern and Tschalenko (1967), who documented the microscopic structure of shear-bands in kaolin specimens in direct shear tests. According to this publication, whatever we assume for the equivalent shear-band thickness, we conclude that this has to be in the order of few hundreds of microns, and suggest a factor of 200 between particle size and shear-band thickness, $d_B \approx 200d_{50\%}$. If we adopt this estimate with $d_{50\%} = 0.007 \text{ mm}$ we end

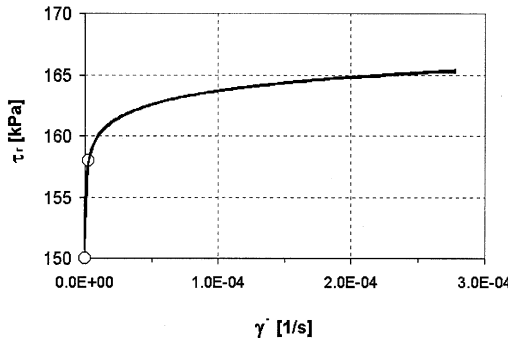


Fig. 3. Strain-rate sensitivity of remolded kaolin clay after Leinenkugel (1976) ($\tau_{\text{ref}} = 158$ kPa, $\dot{\gamma}_{\text{ref}} = 2.8 \times 10^{-6}$ s $^{-1}$, $N = 0.01$).

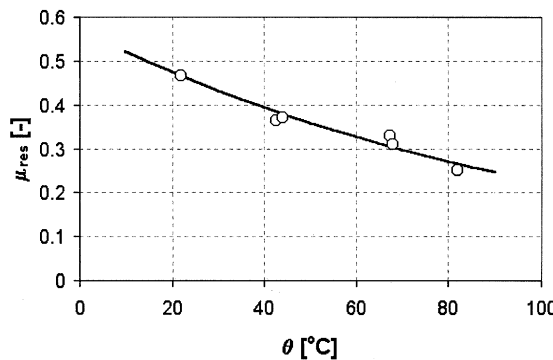


Fig. 4. Thermal friction softening of 'black' (kaolinite) clay: the variation of the critical friction coefficient with temperature, after Hicher (1974).

up here with an estimated shear-band thickness $d_B \approx 1.4$ mm. The assumed upper bound is justified if we assume that the active fault thickness is evolving with fault displacement (cf. Otsuki, 1978; Waterson, 1986; and Drescher et al., 1990).

With these remarks we may re-write Eq. (33) as

$$\beta = \frac{1}{4} \left(\frac{d}{d_{\text{ch}}} \right)^2 \quad (39)$$

with d_{ch} being a characteristic length of the problem, defined as

$$d_{\text{ch}} = \sqrt{\tau_d / \left(\frac{N}{M} j k_m \dot{\gamma}_0 \right)} \quad (40)$$

We observe at this point that in most geologic settings the shear stress τ_d acting on a 'active' fault is related to the depth h_{ref} and to the dip angle δ of the considered fault. As an example we indicate schematically in Fig. 5 'Section 5' of the Vaiont slide of October 9, 1963 after Hendron and Patton (1985). From such a section we get a fair estimate of the shear stress $\tau_d \approx \gamma' h_{\text{ref}} \tan \delta$, acting on a gently dipping fault at relatively shallow depths.

Summarizing the above discussion we conclude that the Gruntfest number β will vary inversely proportional to the depth and dip of the fault, proportionally to the square of the shear-band thickness and proportionally to the thermal softening exponent M ,

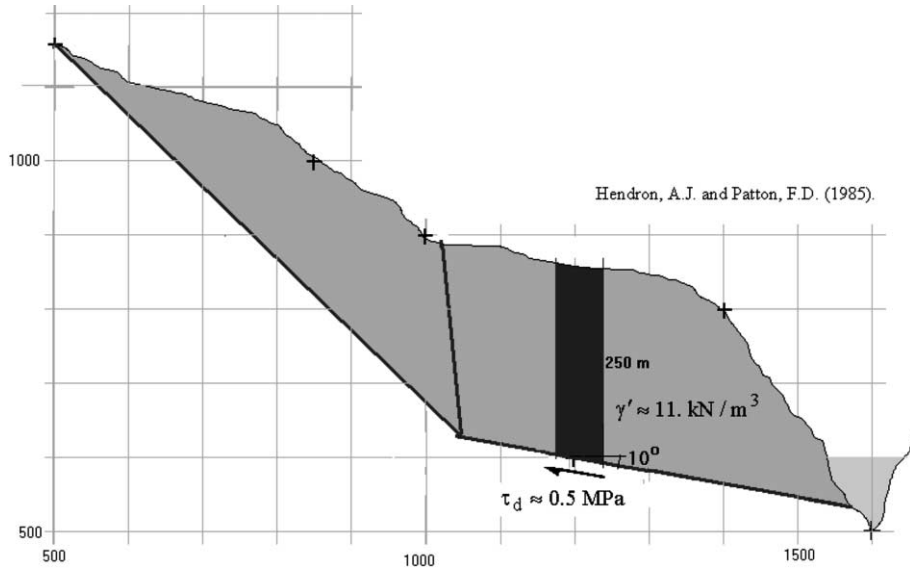


Fig. 5. Critical block failure-mechanism for 'Section 5' of the Vajont slide of October 9, 1963 (cf. Hendron and Patton, 1985).

$$\beta \propto \frac{Md^2}{h_{\text{ref}} \tan \delta} \quad (41)$$

For the assumed range of variation for the exponent ratio $m = M/N$, of the shear-band thickness d and for a reference value for the in situ shear stress of $\tau_d = 1$ MPa we get that the Gruntfest number of the problem is estimated as follows:

- for $d = 0.15$ mm, $m = 1$ $^{\circ}\text{C}^{-1}$: $\beta_{\min} \approx 10^{-7}$
- for $d = 0.1$ m, $m = 0.1$ $^{\circ}\text{C}^{-1}$: $\beta_{\max} \approx 10^{-3}$

Accordingly we will assume that β is a relatively small number as compared to unity.

5. Thermal run-away instability

For small values of the Gruntfest number β , the above transcendental Eq. (37) becomes

$$\theta_d^* - \theta_{\max}^* + \frac{\beta}{2} e^{\theta_{\max}^*} + \mathcal{O}(\beta^2) = 0 \quad (42)$$

The solution of this equation is given in terms of the Lambert W_0 -function³, which satisfies the following functional relationship,

$$W(x) \exp(W(x)) = x \quad (43)$$

We notice that the Lambert W -function has an order two branch point at $x = -e^{-1}$. This means that Lambert $W(x)$ is real-valued and monotonously increasing for x in the range $[-e^{-1}, +\infty]$ and is denoted by W_0 .

³ The notation hereafter follows the paper by Corless et al. (1996); cf. Barry et al. (2000) and Appendix A.

Actually by setting

$$x = \frac{\beta}{2} e^{\theta_d^*} \quad (44)$$

and

$$\theta_{\max}^* = \theta_d^* - W_0(-x) \quad (45)$$

Eq. (42) reduces to the functional relationship (43),

$$W_0(-x) \exp(W_0(-x)) = -x \quad (46)$$

Thus the only analytic at zero solution of Eq. (42) is

$$\theta_{\max}^* = \theta_d^* - W_0\left(-\frac{\beta}{2} e^{\theta_d^*}\right) \quad (47)$$

According to Eq. (47) the critical (maximum) value for the dimensionless ambient temperature corresponds to the branch point of the Lambert W -function; i.e. for

$$-\frac{\beta}{2} e^{\theta_{d,cr}^*} = -e^{-1} \Rightarrow \theta_{d,cr}^* = \ln\left(\frac{2}{\beta}\right) - 1 \quad (48)$$

With

$$W_0(-e^{-1}) = -1 \quad (49)$$

From Eqs. (47) and (48) we get

$$\theta_{\max,cr}^* = \ln\left(\frac{2}{\beta}\right) \quad (50)$$

Notice that the quality of the approximate analytical solution, Eqs. (48) and (50), holding for small values of the Gruntfest number β , was tested numerically.

6. Remark

As pointed out to the author by the reviewer of this paper one may arrive directly to the above results, Eqs. (48) and (50) by a simple geometric interpretation of Eq. (39) written as

$$\frac{\beta}{2} e^{\theta_{\max}^*} = \theta_{\max}^* - \theta_d^* \quad (51)$$

Thus solving Eq. (51) is about finding the intercept of a straight line with an exponential. There might be either two real solutions or none. Above analysis has shown that only one of these solutions is meaningful and that the critical value for θ_d^* is that for which the two solutions coincide, i.e. for which the straight line is tangent to the exponential. A necessary condition is that the derivatives of the right- and left-hand side of the above equation coincide. Therefore we get

$$\frac{\beta}{2} e^{\theta_{\max}^*} = 1 \quad (52)$$

from which indeed Eqs. (50) and (48) follow directly.

It should be pointed out however that this elegant geometric interpretation does not really free us from the use of the not so well-known Lambert W -function. This is the case when we want to compute the temperature and velocity distributions inside the shear-band for values of the ambient temperature which are less than the critical one (see next section).

7. Numerical results and discussion

In Figs. 6 and 7 we show the temperature distribution and the corresponding velocity profile near the critical condition Eq. (48) and for $\beta = 10^{-7}$ ($\theta_{\text{cr}} = 37.8$ °C). We remark that from Eq. (26) we get that shear strain-rate in the shear-band is an exponential function of the dimensionless temperature

$$\dot{\gamma} = \dot{\gamma}_0 e^{\theta^*} \quad (53)$$

The velocity field is derived from this expression by simple numerical integration

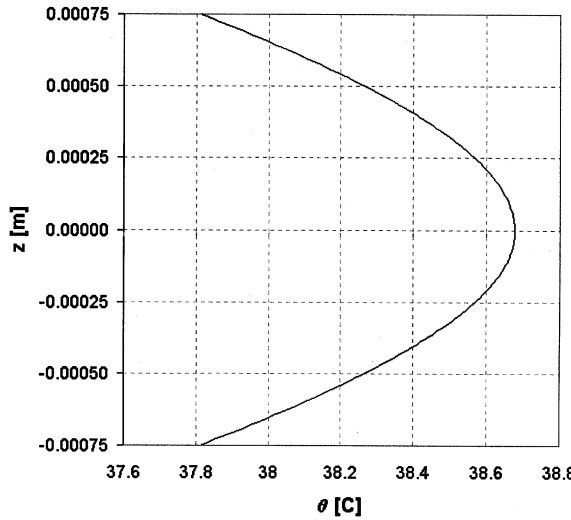


Fig. 6. Temperature profile inside the shear-band near the critical condition ($\beta = 10^{-7}$, $\theta_{\text{cr}} = 37.8$ °C).

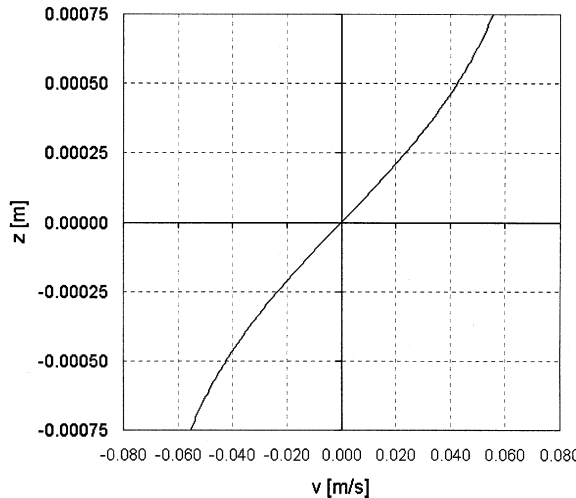


Fig. 7. Velocity profile inside the shear-band near the critical condition ($\beta = 10^{-7}$, $\theta_{\text{cr}} = 37.8$ °C).

$$v^* = \frac{v}{v_0} = \int_0^{z^*} \exp(\theta^*(\zeta)) d\zeta, \quad v_0 = \frac{d}{2} \dot{\gamma}_0 \quad (54)$$

We observe that the boundary velocity increases exponentially with the ambient temperature, reaching ‘catastrophic’ values near the critical temperature (Fig. 8). This result means that above the critical temperature $\theta_{d,cr}$, steady (creeping) shear is not possible, and that the process must evolve dynamically. Thus the present analysis has shown that, for thermally softening, visco-plastically hardening clays, catastrophic shear events may be caused by an increase of the ambient temperature above the problem-specific critical value $\theta_{d,cr}$, given here in dimensionless form by Eq. (48).

Finally, as it can be seen from Fig. 9 the most critical parameter in the analysis is the thermal softening exponent M that sets the range of critical ambient temperatures. In other words this phenomenon is expected to be critical for clays showing pronounced frictional thermal softening (M relatively large).

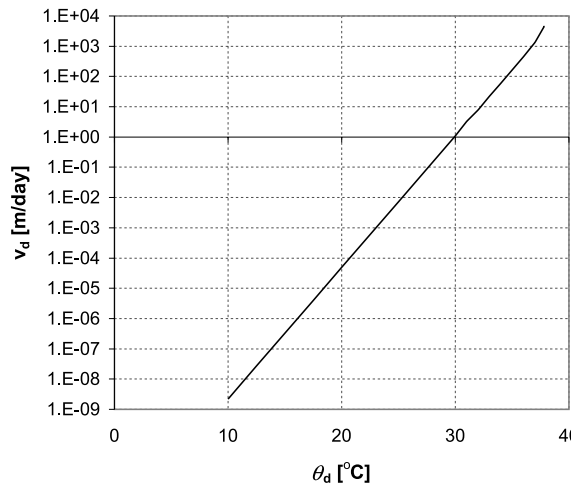


Fig. 8. Boundary velocity as function of ambient temperature ($\beta = 10^{-7}$, $\theta_{cr} = 37.8$ °C).

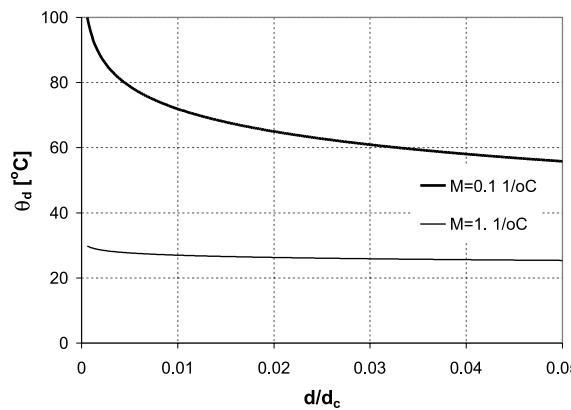


Fig. 9. Variation of the critical ambient temperature for thermal run-away with fault thickness and the exponent M , which determines the sensitivity of the clay towards changes in temperature (frictional thermal softening).

This result could have some bearing in the design of nuclear waste disposal facilities in fissured clayey deposits.

Acknowledgements

The author wants to acknowledge the EU project: Fault, Fractures and fluids: Gulf of Corinth, in the framework of program energy (ENK6-2000-0056).

Appendix A

We are interested in the branch W_0^- of the Lambert function defined in the interval

$$-e^{-1} \leq x \leq 0 : \quad -1 \leq W_0^- \leq 0 \quad (\text{A.1})$$

According to Barry et al. (2000) this branch is approximated as follows (Fig. 10)

$$\begin{aligned} e &= \exp(1) \\ \eta &= 2 + 2ex \\ N_2 &= 3\sqrt{2} + 6 - \frac{((2237 + 1457\sqrt{2})e - 4108\sqrt{2} - 564)\eta}{(215 + 199\sqrt{2})e - 430\sqrt{2} - 796} \\ N_1 &= \left(1 - \frac{1}{\sqrt{2}}\right)(N_2 + \sqrt{2}) \\ W_0^- &= -1 + \frac{\sqrt{\eta}}{1 + \frac{N_1\sqrt{\eta}}{N_2 + \sqrt{\eta}}} \end{aligned} \quad (\text{A.2})$$

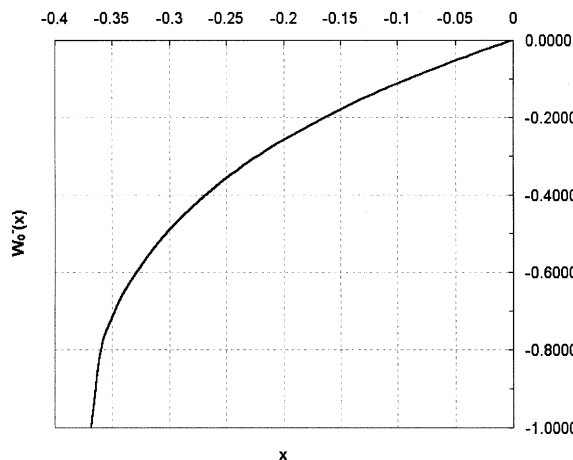


Fig. 10. The Lambert W_0^- -function, Eq. (A.2) after Barry et al. (2000).

References

Adachi, T., Oka, F., 1982. Constitutive equations for normally consolidated clays based on viscoplasticity. *Soils Found.* 22, 57–70.

Anderson, D.L., 1980. An earthquake induced heat mechanism to explain the loss of strength of large rock and earth slides. In: International Conference on Engineering for Protection from natural disasters, Bangkok.

Barry, D.A., Parlange, J-Y., Li, L., Prommer, H., Cunningham, C.J., Stagnitti, F., 2000. Analytical approximations for real values of the Lambert W -function. *Math. Comput. Simulat.* 53, 95–103.

Bishop, A.W., Skinner, A.E., 1977. The influence of high pore-pressure on the strength of cohesionless soils. *Trans. Roy. Soc. London* 284, 91–130, see also reference made therein of Bishop (1953).

Campanella, R.G., Michell, J.K., 1968. Influence of temperature variations on soil behavior. *J. Soil Mech. Found. Div. ASCE* 94, 709–734.

Corless, R.M., Connet, G.H., Hare, D.E.G., Jeffrey, D.J., Knuth, D.E., 1996. On the Lambert W -function. *Adv. Comput. Math.* 5, 329–359.

Despax, D., 1976. Influence de la température sur les propriétés des argiles saturées. Doctoral Thesis, Ecole Centrale de Paris.

Drescher, A., Vardoulakis, I., Han, C., 1990. A biaxial apparatus for testing soils. *Geotech. Testing J.*, GTJODJ 13, 226–234.

Gruntfest, I.J., 1963. Thermal feedback in liquid flow: plane shear at constant stress. *Trans. Soc. Rheol.* 7, 195–208.

Habib, P., 1967. Sur un mode de glissement des massifs rocheux. *C. R. Hebd. Séanc. Acad. Sci. Paris* 264, 151–153.

Hendron, A.J., Patton, F.D., 1985. The Vajont slide, a geotechnical analysis based on new geologic observations of the failure surface. Technical Report GL-85-5. Washington, DC, Department of the Army US Corps of Engineers.

Hicher, P.-Y., 1974. Etude des propriétés mécaniques des argiles à l'aide d'essais triaxiaux, influence de la vitesse et de la température, Report of the soil mechanics laboratory, Ecole Central, de Paris.

Hueckel, T., Baldi, G., 1990. Thermo-plasticity of saturated soils and shales: constitutive equations. *J. Geotechnol. Eng.* 116, 1765–1777.

Laloui, L., 2001. Thermo-mechanical behavior of soils. In: Charlier, R., Gens, A. (Eds.), Environmental Geomechanics, Revue française de génie civil, Vol. 5, No 6, pp. 809–843.

Kamke, E., 1977. Differentialgleichungen, Vol. I, Chapter 6, Section 6.76, p. 562, Teubner.

Leinenkugel, H.-J., 1976. Deformations- und Festigkeitverhalten bindiger Erdstoffe. Experimentelle Ergebnisse und ihre physikalische Deutung, Dissertation, Univ. Karlsruhe, Heft 66.

Mase, C.W., Smith, L., 1985. Pore-fluid pressures and frictional heating on a fault surface. *Pageoph* 122, 583–607.

Modaressi, H., Laloui, L., 1997. A thermo-viscoplastic constitutive model for clays. *Int. J. Num. Anal. Meth. Geomech.* 21, 313–335.

Morgenstern, N.R., Tschalenko, J.S., 1967. Microscopic structures in kaolin subjected to direct shear. *Geotechnique* 17, 309–328.

Nova, R., 1986. Soil models as a basis for modelling the behaviour of geophysical materials. *Acta Mech.* 64, 31–44.

Otsuki, K., 1978. On the relationship between the width of the shear zone and the displacement along the fault. *J. Geol. Soc. Jpn.* 84, 661–669.

Sigh, A., Mitchell, J.K., 1968. General stress-strain-time function for soils. *J. ASCE/SMFD* 94 (SM1), 21–46.

Taylor, D.W., 1948. Fundamentals of Soil Mechanics. Wiley, New York.

Tika, Th.E., Hutchinson, J.N., 1999. Ring shear tests on soil from the Vajont landslide slip surface. *Geotechnique* 49, 59–74.

Vardoulakis, I., 2000. Catastrophic landslides due to frictional heating of the failure plane. *Mech. Coh.-Frict. Mater.* 5, 443–467.

Vardoulakis, I., 2002. Dynamic thermo-poro-mechanical analysis of catastrophic landslides. *Géotechnique*, in press.

Vardoulakis, I., Sulem, J., 1995. Bifurcation Analysis in Geomechanics. Blackie Academic and Professional, London.

Voight, B., Faust, C., 1982. Frictional heat and strength loss in some rapid landslides. *Géotechnique* 32, 43–54.

Waterson, J., 1986. Fault dimensions, displacement and growth. *Pageoph* 124, 365–373.

Yu, C.-J., Sultan, N., Delage, P., 1999. A thermomechanical model for saturated clays. *Can. Geotechnol. J.* 37, 607–620.